Monthly Notices of the ROYAL ASTRONOMICAL SOCIETY

Mon. Not. R. Astron. Soc. **426,** 816–832 (2012) doi:10.1111/j.1365-2966.2012.21445.x

STEREO observations of long period variables

K. T. Wraight,[1⋆] D. Bewsher,[2] Glenn J. White,[1,3] W. Nowotny,[4] A. J. Norton[1] and C. Paladini[4]

[1]*Department of Physical Sciences, The Open University, Milton Keynes MK7 6AA*
[2]*Jeremiah Horrocks Institute, University of Central Lancashire, Preston, Lancashire PR1 2HE*
[3]*Space Science and Technology Department, STFC Rutherford Appleton Laboratory, Chilton, Didcot, Oxfordshire OX11 0QX*
[4]*Department of Astronomy, University of Vienna, Türkenschanzstrasse 17, 1180 Vienna, Austria*

Accepted 2012 June 4. Received 2012 May 28; in original form 2012 April 4

ABSTRACT

Observations from the Heliospheric Imagers (HI-1) on both the *STEREO* spacecrafts have been analysed to search for very long period large amplitude stellar variability, finding six new candidates. A total of 85 objects, mostly previously known Mira variables, were found to show convincing variability on time-scales of over a 100 days. These objects range in peak brightness from about fourth magnitude to 10th magnitude in *R* and have periods between about 170 and 490 d. There is a period gap between 200 and 300 d where no objects were found and this is discussed. 15 of the Miras in the sample are previously recorded as having variable periods and the possibility for these and two other stars to have undergone a period change or to be irregular is discussed. In addition to the six stars in the sample not previously recorded as variable, another seven are recorded as variable but with no classification. Our period determination is the first to be made for 19 of these 85 stars. The sample represents a set of very long period variables that would be challenging to monitor from the Earth, or even from Earth orbit, owing to their position on the ecliptic plane and that their periods are often close to a year or an integer fraction thereof. The possibility for the new candidates to possess circumstellar shells is discussed.

Key words: techniques: photometric – catalogues – stars: AGB and post-AGB – stars: late-type – stars: oscillations.

1 INTRODUCTION

Roughly 400 years ago, the first variable star was recognized due to its changing brightness (Hoffleit 1997). This red object, showing striking light variations in the visual, was later named o Cet and became the first member of the variability class called long period variables (LPVs) today. Being easily detectable because of the large photometric amplitudes, they were intensively studied thereafter and represent now a prominent group within the General Catalogue of Variable Stars (GCVS; Samus et al. 2012). It is known nowadays that LPVs are stars of low to intermediate main-sequence mass ($\approx$0.8–8 $M_{\odot}$) in a quite late stage of stellar evolution, the asymptotic giant branch (AGB). Such late-type giants populate regions of high luminosities (several 10^3 $L_{\odot}$) and low effective temperatures (below $\approx$4000 K) in the Hertzsprung–Russell diagram. During the AGB evolution, the stars start to pulsate which causes the pronounced photometric variations (e.g. Olivier & Wood 2005). Conventionally, LPVs were subclassified into Miras, semiregular variables and irregular variables with the visual amplitude and the regularity of the light curve as criteria. An important step forward in our understanding of LPVs was provided by the large surveys of the Magellanic Clouds and the Galactic bulge (e.g. Wood 2000; Ita et al. 2004; Groenewegen & Blommaert 2005; Matsunaga, Fukushi & Nakada 2005), recently updated with space-based infrared (IR) data (Riebel et al. 2010). From these, we know that AGB variables constitute a few period–luminosity (PL) relations. The most prominent LPVs, namely the Mira variables, can be found along the sequence for fundamental mode pulsators. The majority show large amplitude variations (ΔV of a few magnitudes, $\Delta K \approx 0.4$–1 mag) on time-scales of 100–600 d (e.g. Whitelock, Marang & Feast 2000). The PL relation for Miras was determined rather precisely based on a number of well-characterized Large Magellanic Cloud objects by Whitelock, Feast & van Leeuwen (2008) but could be investigated also in other Local Group galaxies (e.g. Lorenz et al. 2011) and even in systems as distant as Cen A (Rejkuba 2004). Apart from pronounced mass loss (e.g. Nowotny et al. 2011), AGB stars are also characterized by the occurrence of He-shell flashes (thermal pulses; Lattanzio & Wood 2004). Not only are these responsible for changing the atmospheric chemistry from O rich to C rich via dredge-up of carbon from the interior, but also thermal pulses are suspected to be the reason for period changes in observed light curves (e.g.

⋆E-mail: k.t.wraight@open.ac.uk

Templeton, Mattei & Willson 2005; Lebzelter & Andronche 2011; Uttenthaler et al. 2011).

The data used in this study come from NASA's *STEREO* mission, which aims to image the Sun's corona in three dimension and observe coronal mass ejections from the surface of the Sun out to the Earth's orbit (Kaiser et al. 2008). The two satellites are in different heliocentric orbits, one slightly inside the Earth's orbit (*STEREO*-Ahead) and one slightly outside (*STEREO*-Behind) and the angle between each satellite, the Sun and the Earth increases by about 22.°5 every year. Photometry of background stars in the images is possible as the calibration of the Heliospheric Imager (HI) cameras has been performed to a very high standard (Brown, Bewsher & Eyles 2009; Bewsher et al. 2010; Wraight et al. 2011, 2012; Bewsher, Brown & Eyles 2012). Having two nearly identical satellites in different heliocentric orbits provides greater phase coverage of LPVs, with greater homogeneity than achievable from observations conducted from the ground.

In the following sections, we outline the characteristics of the *STEREO*/HI-1 observations and explain how the sample was extracted and analysed. We provide periods for 85 stars showing large amplitude variability ($\geq$0.3 mag) with periods longer than 100 d. The majority of these are known to be Miras or semiregular variables. We estimate times of maximum brightness, where visible. Our analysis of patterns found in the sample focuses on the errors obtained for the periods and also on a gap in the periods found between 200 and 300 d. We discuss a number of individual stars, in particular those which are known to have varying periods, those which have not previously been classified and those found here to be variable for the first time.

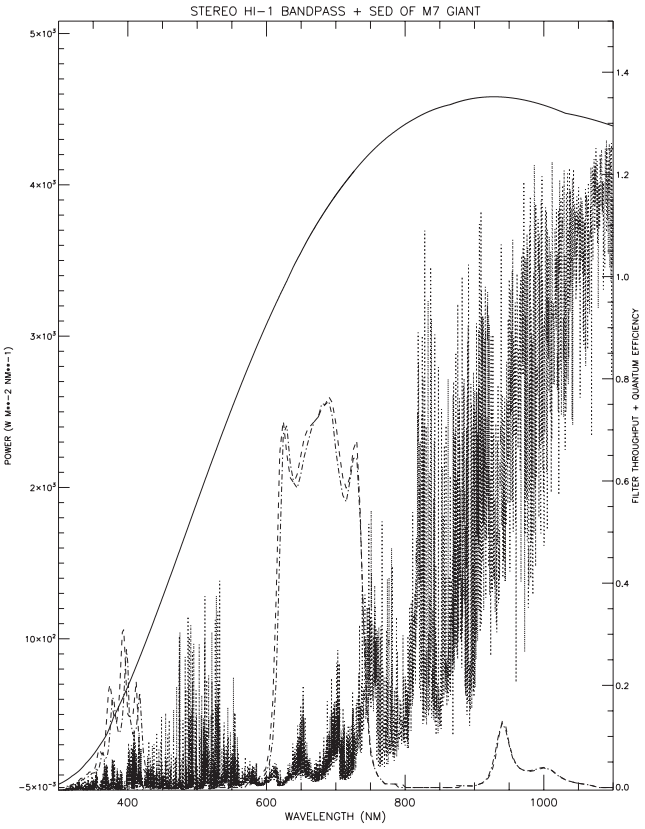

Figure 1. Plot of the filter throughput convolved with the quantum efficiency of the CCDs for *STEREO*/HI-1A, shown in a dashed line [*STEREO*/HI-1B is almost identical (Bewsher et al. 2010), shown here in a dot–dashed line]. This is set against a synthetic spectral energy distribution of a red giant with MK spectral type M7 (Fluks et al. 1994), shown in a dotted line, with the continuum emission in a solid line.

2 OBSERVATIONS AND ANALYSIS

2.1 Characteristics of *STEREO*/HI-1 observations

The HIs are described in detail in Eyles et al. (2009) but we summarize the main features here for convenience. The field of view of the *STEREO*/HI-1 cameras is $20^\circ \times 20^\circ$, centred 14° away from the Sun's centre. The aperture of the cameras is just 16 mm and the focal length is 78 mm. Each CCD is 2048 $\times$ 2048 pixel, which provides a plate scale of 35 arcsec pixel^{-1}. The images are binned 2 $\times$ 2 on-board, to reduce the bandwidth, and as a result the final images received have a resolution of 70 arcsec pixel^{-1}. Each image is the result of 30 summed exposures, with each exposure lasting 40 s, and one image is produced every 40 min. In this way, stars as faint as 12th magnitude in *R* can be observed but only the very brightest stars will saturate the CCDs. Stars of about fourth magnitude may show some systematic effects due to saturation, whilst third magnitude stars often show systematic effects but may be usable, whereas stars of second magnitude and brighter are unusable. We use the NOMAD1 catalogue (Zacharias et al. 2004) to determine which stars to observe, selecting all those listed as 12th magnitude or brighter in the *R* band within our field of view. Aperture photometry is performed on each star as described in Bewsher et al. (2010) and the data reduction pipeline is summarized in Wraight et al. (2011). This provides an extremely useful resource, with photometry of almost 900 000 stars along the ecliptic plane.

The *STEREO*/HI-1 imagers have an unusual spectral bandpass (Fig. 1). They are most sensitive in between 630 and 730 nm but also have some sensitivity in the blue, around 400 nm, and in the IR at around 950 nm. The sensitivity in the blue is very useful for observing hot stars (Wraight et al. 2012) but it is the sensitivity in the IR that makes the observations of many of the very cool stars in this paper possible. Some of the stars in our sample are cool enough, or sufficiently obscured by circumstellar material, to be fainter than 12th magnitude in the *R* band and do not feature in the *STEREO* data base directly. In these cases, the large pixel size of the *STEREO*/HI-1 imagers, combined with the sensitivity near 950 nm, allows them to be observed indirectly through blending with a nearby star that is in the data base. As Mira variables are known to change their temperature and spectral type, the magnitude of the variability observed by *STEREO*/HI-1 is not reliable. This can be seen by referring to synthetic spectra of red giants (Fluks et al. 1994). There is a significant difference in the emission in the region 630–730 nm between the spectral type M6, where there is still some emission, and M7 and later, where there is relatively little emission. A star varying across this threshold will therefore have an exaggerated amplitude. Giants of spectral type M7 or later are seen almost entirely through their emission in the IR and may show different variability to that seen in other parts of the spectrum, whilst giants of M6 and earlier may show variability due to processes affecting both the red and the IR. In particular, it is worth noting that some of the faintest stars in our sample, including many of the new candidates, are so faint that only deep all-sky surveys, e.g. Zacharias et al. (2004) and Monet et al. (2003), have detected them in visible light. Even in the IR observations are scarce, mostly from the *IRAS* mission (Neugebauer et al. 1984), the *Akari* mission

(Murakami et al. 2007) and in the Two Micron All-Sky Survey (2MASS) (Skrutskie et al. 2006).

2.2 Quality of *STEREO*/HI-1 data

In order to determine a period for the candidate variables, it was necessary to use undetrended data and the only processing that was applied was the exclusion of obvious outliers and systematics, where possible. This is because the polynomial detrending normally used to clean the light curves removes long period variability. As a result, many of the light curves show indications of artificial trends, often a result of the flat-fielding breaking down near the edges of the detectors. Other sources of noise affect the long period signals being searched for to a lesser degree, most notably de-pointing events associated with micrometeorite hits, which are more common in the data from the *STEREO*-Behind satellite, *STEREO*/HI-1B, also observed by Davis et al. (2012). The presence of artificial trends and the ability to recognize them as such also limit the number of maxima that can be reliably observed for the stars in the sample and might also influence the times of maximum light, in those cases where the effect is small enough to be reasonably sure a maximum is genuinely being observed.

2.3 Data analysis

In order to extract the sample, the first step was to select those stars showing the largest difference in the weighted mean magnitude observed by the two satellites. We anticipated that the majority of these would be due to systematic effects, mostly relating to flat-fielding near the edges of the CCDs but also due to planetary incursions from Venus and Mercury which frequently pass through the field of view. The photometry is also conducted very slightly differently between the two imagers, using aperture photometry with different apertures (Bewsher et al. 2010). As a result, there are differences between the weighted mean magnitudes observed by the two satellites, with these systematics being greatest in the Galactic Centre and anti-centre. In normal circumstances, however, the magnitude of these differences amounts to less than 50 mmag and experience has found empirically that systematics are not significant unless the magnitude of the difference between the two satellites is larger than 0.1 mag. In contrast, the smallest such difference of any object included in the sample is that of V901 Sco, a known semiregular variable, which in *STEREO*/HI-1 shows a difference of slightly over 0.3 mag between the two satellites and is unlikely to be due solely to systematic effects. The presence of these systematics is the reason why Miras especially were searched for, as their variability is so large with respect to this background noise that misidentifications are relatively unlikely. Approximately 10 000 light curves were visually examined showing large differences in the weighted mean magnitudes between the two satellites, from which a sample of about 130 was recovered that appeared to be more likely due to genuine variability than any known systematic effects. The possibility of this process introducing a selection effect is discussed after the results have been presented, as it is one possible cause for a lack of any objects in the sample showing a periodicity between 200 and 300 d. For every one of these stars, some basic information was extracted from the SIMBAD data base and the NOMAD1 catalogue (Zacharias et al. 2004), so as to identify the source of the variability observed. In many cases, especially in the Galactic Centre, it was not possible to be reasonably sure of the origin of the observed variability, mostly because there were too many candidates but often because there were no candidates showing the colours expected of a red giant.

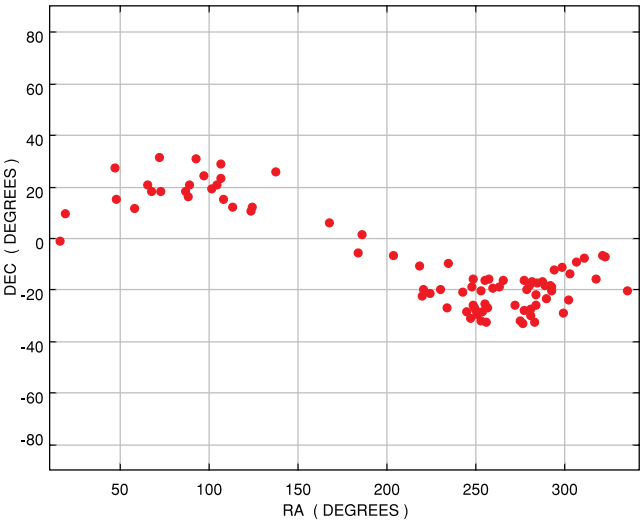

Figure 2. Plot of the locations of the 85 stars in the sample on the sky, with RA and Dec. given in degrees. As *STEREO*/HI-1 only observes stars within 10° of the ecliptic plane, this is where the candidates are found. Note that more are observed near to the Galactic Centre.

A few were deselected after further examination showed that systematics were more likely responsible for the variability, or because a period could not be found during the final stage of the analysis. A sample of 85 was eventually analysed in detail using PERANSO[1] and a period determination made using a discrete Fourier transform (DFT; Deeming 1975), phase dispersion minimization (PDM; Stellingwerf 1978) and the Renson string length minimization (SLM) method (Renson 1978). Although PERANSO has numerous algorithms implemented, these three have a fundamentally different basis to each other and are expected to have different, hopefully complementary, strengths and weaknesses. It was important for the methods chosen to be able to deal with a very small number of data points, as each epoch of about 20 d would effectively be treated like a single point. The ability to straightforwardly and manually remove known, obvious, artefacts, such as planetary incursions due to Venus and Mercury passing through the field of view, made PERANSO preferable to other programs, at the expense of being slightly more time consuming, which was why using numerous additional algorithms was not done. The median value found by the three algorithms was used, so that if any two algorithms agreed this would produce a more reliable period. This produced a proportional difference between the periods found and the previously known periods of about 4 per cent (Section 3.1). Periods were searched for in the range of 50–1000 d and the strongest signal of each of the three different algorithms was recorded, along with the error. Where possible, times of maxima were also recorded along with the corresponding magnitude observed. These periods and ephemerides are one of the main results of the research presented herein, along with the photometry presented in the form of light curves phase folded on these periods. The location of the 85 stars in the sample on the sky is shown in Fig. 2. As an example of a bright well-known Mira, we show the undetrended data and the phase-folded light curve for R Cnc along with the periodogram from a DFT analysis of these data in Fig. 3.

[1] http://www.peranso.com

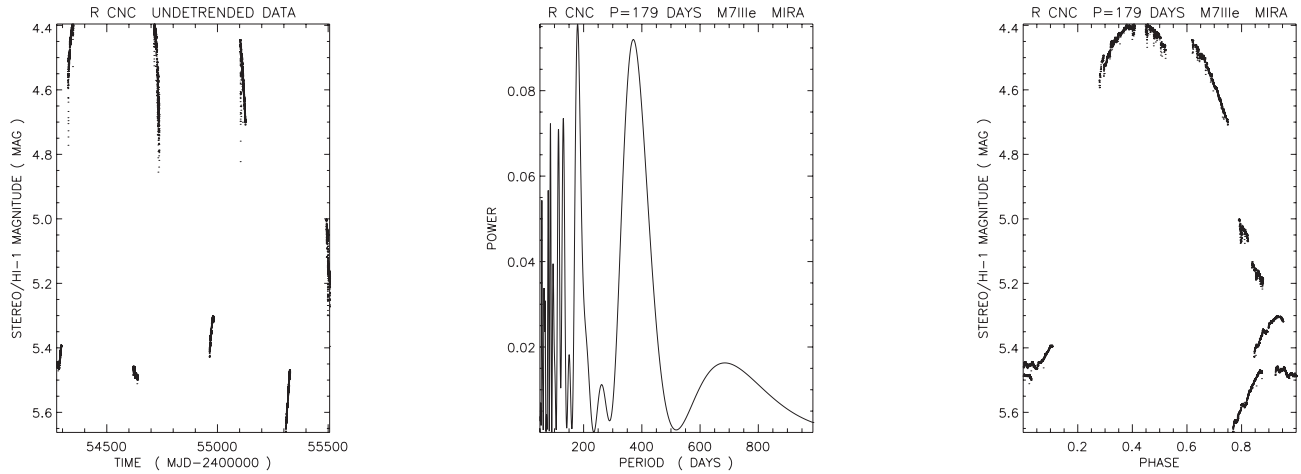

Figure 3. The known Mira variable R Cnc, as observed by *STEREO*/HI-1. The raw light curve is shown on the left, the DFT of this light curve after culling of outliers is then shown in the middle plot and the phase-folded light curve on the strongest period (179 d) is shown on the right. Note that the known period of this well-observed star is 361.6 d (Samus et al. 2012).

3 RESULTS

The analysis produced periods, with errors, for 85 stars and the time of at least one maximum for 24 of these (Table 1) but V932 Sco was excluded from the table as it is a known Orion[2] variable and the table is likely to be used as a resource for bright LPV stars. This is the first period determination for 19 of these 85 stars, seven of which were previously unclassified and six previously unknown to be variable. Table 2 shows when the six previously unknown candidate variables will next be observed by *STEREO*/HI-1. The phase-folded light curves of all 85 stars on the periods found are given in Appendix A (Figs A1–A5; see Supporting Information). Unfolded light curves for some stars of interest are also shown (see Section 4). V932 Sco has no period given in Samus et al. (2012) and the period found here of 423 ± 87 d is the first determination of a period; however, no maxima were observed. As it is important to remind the reader that there is a chance that the new variables (marked with '–' in column 11 of Table 1) and the unclassified variables (marked as V* in column 11 of Table 1) are not necessarily Miras or semiregular variables, V932 Sco has otherwise been retained in the sample.

Table 1 shows the available information for each of the 84 stars (V932 Sco, a known Orion variable, was excluded so as to provide a list of known and probable LPV stars) and lists the name of the known or candidate variable, the name of the star observed by *STEREO*/HI-1 where this is different from the star believed to be the origin of the variability, the right ascension and declination (in degrees) of the star observed by *STEREO*/HI-1, the period found from the analysis of the *STEREO*/HI-1 light curve (in days), the error given for this period by Peranso (in days), which algorithm produced this period (1 for PDM, 2 for DFT or 3 for SLM), the period given by SIMBAD (NA is shown if none is available) – preferentially the GCVS (Samus et al. 2012), whether the GCVS notes that the period has been observed to vary, the spectral type given by SIMBAD, the variability type given in the GCVS [including the New Suspected Variable (NSV) supplement, these are marked as such], where known, followed by the Modified Julian Date (MJD) of all maxima observed in the *STEREO*/HI-1 photometry, a visual estimate of the error in this time (in days) and the *STEREO*/HI-1 magnitude of each maxima. If a spectral type determination has not been made or the star has not previously been recorded as variable, then '–' is used to denote the absence of these data.

The sample of 85 stars for which a period was determined were analysed for trends in their periods. Some of this analysis was done using R[3] (R Development Core Team 2008) and some using TOPCAT.[4] The main reason for doing this was that the errors returned for the periods by Peranso were often very large and it was necessary to verify whether they were valid. Secondly, there were no stars in the sample for which the best period found was between 200 and 300 d, which was not expected. All these 85 stars were also checked for known periods in SIMBAD, the GCVS (Samus et al. 2012) period being used preferentially where multiple determinations were available. The actual *STEREO*/HI-1 images of several stars were examined showing maximum and minimum brightness in order to ascertain that even from a distance of 2 or 3 pixel, some of the stars in the sample could still have been observed indirectly (e.g. Y Sco, shown in Fig. 4).

3.1 Trends in the data

The concern regarding the accuracy of the errors in the periods returned by Peranso is demonstrated by Figs 5–7. The large size of the errors implies that the algorithms were, individually, struggling to resolve a signal; however, comparing the median period of the three algorithms with the known periods from the GCVS (Samus et al. 2012) shows that a more appropriate 1σ error bar for the entire sample is 4 per cent (Fig. 8). A direct plot of the median period found here against the GCVS periods shows a few cases where harmonics may have been found by *STEREO*/HI-1 instead of the correct period but confirms the overall good match (Fig. 9). Table 1 gives all the median periods and other information of relevance for each star in the sample. Light curves phase folded on these periods are also given in Appendix A (see Supporting Information).

There are no periods found between 200 and 300 d in the sample, as shown in the right-hand panel in Fig. 10. This is in contrast to

[2] Orion variables are very young stars that have not yet joined the main sequence and show large amplitude irregular variability.

[3] http://www.R-project.org

[4] http://www.starlink.ac.uk/topcat/

Table 1. 84 stars showing long period variability in *STEREO*/HI-1 data. V932 Sco was excluded from the table as it is a known Orion variable and the new and unclassified variables are more likely to be Miras or semiregular variables, making this table a resource of known and probable LPV stars.

Star name	Star observed by *STEREO*/HI-1	RA (°)	Dec. (°)	*STEREO*/HI-1 period (d)	*STEREO*/HI-1 period error (d)	Algorithm (1 = PDM 2 = DFT, 3 = SLM)	Known period (d)	Period known to vary	Spectral type	GCVS variability type	Maximum (MJD)	± error in maximum (d)	*STEREO*/HI-1 magnitude at maximum
ZCet		016.6880	−001.4814	186	17	2	184.81	0	M5e	Mira	54604.00	2.5	7.18
											54978.00	4.0	7.60
SPsc		019.3939	008.9313	413	149	3	404.62	0	M7e	Mira	54606.35	3.5	6.90
											55386.21	4.0	7.44
ZAri		047.0491	026.9877	341	35	2	337	0	M5	Mira	54557.77	4.0	8.51
UAri		047.7627	014.8001	397	48	2	371.1	0	M5.5e	Mira			
IKTau		058.3702	011.4060	449	216	3	470	0	M6me	Mira			
V1100Tau	NOMAD1 1102−0050892	065.3896	020.2805	331	67	3	NA	0	M6me	Mira			
V718Tau		067.8414	017.6529	396	72	1	405	0	Ce	Mira			
MYAur		072.3385	030.9265	323	47	1	331.6	0	–	Mira			
VTau		073.0096	017.5380	170	8	2	168.7	1	Kp	Mira			
EITau		086.7355	017.9086	360	56	1	364	0	Sv	SR	55280.00	4.0	8.73
ZTau		088.1039	015.7958	438	81	1	466.2	1	S7.51e	Mira			
UOri		088.9549	020.1752	372	65	1	368.3	1	M8III	Mira			
BVAur		092.7280	030.2310	365	44	2	388	0	M8	Mira			
HVGem	TYC 1879-585-1	097.2217	024.0277	369	68	1	386	0	–	Mira			
RTGem		101.6440	018.6149	346	21	2	350.4	0	C	Mira	55479.82	4.5	8.03
IUGem	NOMAD1 1100−0135465	104.3910	020.0554	385	42	2	NA	0	M8e	SR			
RGem		106.8390	022.7035	391	59	2	369.91	0	S2.9e-S8.9e(Tc)	Mira			
AMGem	NOMAD1 1183−0161263	106.7950	028.3008	387	47	2	356.3	0	M10	Mira			
VXGem		108.2040	014.6010	365	50	2	379.4	0	C7.2e-C9.1e(Nep)	Mira			
T CMi		113.5020	011.7353	325	57	1	328.3	1	M5	Mira			
VWCnc	NOMAD1 1001−016333	123.4310	010.1629	382	47	2	366	0	M7	Mira			
RCnc		124.1410	011.7262	179	11	2	361.6	0	M7IIIe	Mira	54978.54	2.0	5.30
WCnc		137.4690	025.2483	399	50	2	393.22	0	M7e	Mira			
SLeo		167.7120	005.4597	197	25	1	190.16	1	M3me	Mira	55172.05	3.5	9.40
											55358.35	4.0	9.15
TVir		183.6530	−006.0358	330	113	3	339.47	0	M6e	Mira			
SSVir		186.3100	000.7697	377	55	2	364.14	1	C	SR	55028.79	3.0	5.27
											55370.93	2.5	5.06
SVir		203.2500	−007.1947	356	56	2	375.1	1	M7IIIe	Mira			
KSLib	NOMAD1 0790−0270584	218.2080	−010.9123	362	46	2	380	0	Me	Mira			
EPLib		219.9990	−022.5740	191	19	1	185.78	0	–	Mira			
SXLib	HD129380	220.6990	−020.2238	324	129	3	332.9	0	M6e	Mira			
EGLib		223.8400	−022.0055	402	378	3	365	0	M5	Mira			
SLib		230.3500	−020.3884	197	24	1	192.9	1	M2	Mira			
SVLib		233.3410	−027.1855	405	101	1	402.66	0	M8+	Mira			
TZLib		234.2140	−010.0802	193	20	1	183.6	0	–	Mira	54462.38	3.0	8.86
											54844.66	4.0	8.72
XSco		242.1330	−021.5305	198	34	1	199.86	0	M2	Mira	55245.09	3.0	9.02
WWSco	NOMAD1 0587−0415805	246.8190	−031.2615	435	86	1	431	0	M9	Mira			
YSco	NOMAD1 0706−0340442	247.3880	−019.3839	355	48	2	351.88	1	M8	Mira	54474.10	2.5	8.82
											55255.82	4.0	8.45
WXSco		248.2020	−026.3850	385	85	1	187.9	0	M6	Mira			
TOph		248.4310	−016.1317	377	45	2	366.82	0	M6.5e	Mira			
XZSco		249.2640	−027.3132	365	50	2	300	0	–	Mira			
YYSco	NOMAD1 0614−0400462	249.5170	−028.5985	379	106	1	327.43	0	M7e	Mira			
CISco	NOMAD1 0602−0420519	250.5110	−029.7392	389	109	1	NA	0	–	V*			

Table 1 – *continued*

Star name	Star observed by *STEREO*/HI-1	RA (°)	Dec. (°)	*STEREO*/HI-1 period (d)	*STEREO*/HI-1 period error (d)	Algorithm (1 = PDM 2 = DFT, 3 = SLM)	Known period (d)	Period known to vary	Spectral type	GCVS variability type	Maximum (MJD)	± error in maximum (d}	*STEREO*/HI-1 magnitude at maximum
IRAS 16482−2039	NOMAD1 0692−0384552	252.8140	−020.7219	376	50	2	NA	0	–	–			
IRAS 16469−3211	NOMAD1 0577−0577145	252.5500	−032.2835	360	48	2	NA	0	–	V*(NSV)			
CROph	NOMAD1 0611−0442400	253.8260	−028.8998	327	74	1	345.7	0	M	Mira			
V1163Oph		254.6800	−016.8690	321	49	1	324	0	–	Mira			
EGOph	NOMAD1 0639−0431340	254.7280	−026.0260	410	79	2	NA	0	–	V*			
V901Sco		255.6910	−032.7255	409	112	3	NA	0	Ne	SR			
GPOph		256.2530	−027.2164	328	83	1	NA	0	M6	SR	54871.96	3.5	8.73
ROph		256.9410	−016.0927	302	127	3	306.5	1	M4e	Mira	55256.71	2.0	5.70
AEOph	NOMAD1 0699−0414346	259.4700	−020.0211	359	49	2	176	0	–	Mira	55444.80	5.0	8.21
IRAS 17289−1917	NOMAD1 0706−0429226	262.9790	−019.3255	171	10	1	NA	0	–	–			
BGOph	NOMAD1 0732−0506383	265.4140	−016.7940	386	56	2	342.5	0	M9	Mira			
IRC −30357	NOMAD1 0635−0722217	271.8500	−026.4031	353	50	2	NA	0	M8	–			
BRSgr		275.0510	−032.2159	309	61	1	302.8	0	M4e	Mira			
V1869Sgr		275.9300	−033.2451	318	35	2	332	1	Me	Mira			
AKSgr		277.005	−016.7509	385	37	2	413.15	0	M5e-M9	Mira			
HRSgr		277.0920	−028.2411	380	46	2	NA	0	–	V*			
V3876Sgr		278.3030	−020.0973	344	87	1	352	1	M8	Mira	54890.57	3.0	8.02
IRC −20507	NOMAD1 0714−0715901	280.0740	−018.5605	431	86	1	NA	0	M7	–	55464.71	5.0	8.55
V3867Sgr	NOMAD1 0595−0911163	280.7240	−030.5022	414	183	3	422	0	–	Mira			
V3878Sgr	NOMAD1 0618−1015599	280.7590	−028.1300	357	45	2	345	0	–	Mira			
V3952Sgr		281.4640	−017.2999	492	153	2	NA	0	M9	Mira	55287.07	5.0	7.61
V2055Sgr		283.0480	−032.8287	321	34	1	320	0	–	Mira			
OPSgr		283.3480	−026.3368	397	47	2	303	0	Me	Mira			
V5545Sgr	NOMAD1 0676−0984820	283.4830	−022.3865	368	46	2	377	0	Me	SR	54506.99	2.5	8.50
											54895.71	3.0	8.35
											55283.38	5.0	8.52
NSV 11552		284.0560	−017.7138	179	16	2	NA	0	–	V*			
FQSgr		286.9030	−017.0215	432	87	1	434	0	M8	Mira	55285.02	5.0	6.89
RXSgr		288.6370	−018.8120	326	87	1	335.23	1	M5e	Mira	54780.85	3.0	7.23
TYSgr		289.4280	−023.9402	324	126	3	325.41	0	M3e	Mira			
ANSgr		291.7610	−018.5139	325	53	3	337.56	1	M5e-M8	Mira			
IRAS 19263−1922		292.3270	−019.2722	386	41	2	NA	0	–	V*(NSV)			
2MASS J19291709−2034504	NOMAD1 0693−0875859	292.3310	−020.6250	425	87	1	NA	0	M7	–			
V360Sgr		293.9280	−012.7919	367	46	2	165	0	M7	SR	54522.44	3.0	9.39
											54905.91	3.0	9.28
											55295.30	5.0	9.71
NOMAD1 0784−0674630		298.3360	−011.5768	381	51	2	NA	0	–	–			
RRSgr		298.9850	−029.1900	335	131	2	336.33	1	M5e	Mira			
IRAS 20060−2425		302.2470	−024.2704	376	376	3	NA	0	–	V*(NSV)			
RCap		302.8260	−014.2676	175	10	2	345.13	0	Cev	Mira	54524.99	3.0	7.53
SWCap		306.5840	−009.5489	363	51	2	344.6	0	M8	Mira			
XXAqr		310.5790	−008.2585	345	37	2	323.4	0	M4	Mira			
ZCap		317.6560	−016.1737	181	17	2	181.48	0	M Iab:e	Mira			
RZAqr		320.7650	−007.1082	429	117	1	391	0	M9	Mira	54549.49	3.5	7.09
HYAqr		322.7770	−007.5723	309	65	1	311	0	M8	Mira	54819.52	3.5	8.86
XAqr		334.6640	−020.9011	306	58	1	311.4	0	S6.3e M4e-M6.5e	Mira			

Table 2. The dates shown (in MJD − 240 0000) in this table are when the six new candidate variables will next be observed by *STEREO*/HI-1. The times take into account the mask that is routinely applied to exclude data likely to be affected by solar activity. As the Sun is going to be at maximum during these observations, it is not expected that observations will be reliable within the region of the CCDs excluded by the mask.

Star name	Star observed by *STEREO*/HI-1	RA (°)	Dec. (°)	Start and end dates of upcoming *STEREO*/HI-1 observations (MJD − 240 0000)			
				STEREO/HI-1A	*STEREO*/HI-1B	*STEREO*/HI-1A	*STEREO*/HI-1B
IRAS 16482−2039	NOMAD1 0692−0384552	252.8140	−020.7219	56119.30339–56131.47135	56418.86914–56432.20117	56463.46094–56475.62891	56807.82813–56821.16016
IRAS 17289−1917	NOMAD1 0706−0429226	262.9790	−019.3255	56129.12500–56142.40234	56428.35156–56441.51953	56473.65234–56486.92969	56817.29688–56830.46484
IRC −30357	NOMAD1 0635−0722217	271.8500	−026.4031	56137.03385–56150.17057	56436.99805–56450.05664	56481.57031–56494.70703	56826.03906–56839.09766
IRC −20507	NOMAD1 0714−0715901	280.0740	−018.5605	56144.72005–56158.02474	56444.58789–56457.72852	56489.23828–56502.54297	56833.54688–56846.68750
2MASS J1929 1709−2034504	NOMAD1 0693−0875859	292.3310	−020.6250	56155.52474–56168.82943	56456.15234–56469.20703	56500.04297–56513.34766	56845.20703–56858.26172
NOMAD1 0784−0674630		298.3360	−011.5768	56162.64714–56182.14714	56456.62109–56476.50781	56507.15625–56526.65625	56845.66406–56865.55078

Figure 4. ESO *R*-band image centred on the Mira variable Y Sco (left), *STEREO*/HI-1A image showing the same field of view near minimum (middle) and *STEREO*/HI-1B image of the same field of view at maximum (right). The nearby bright star is NOMAD1 0706−0340442 and is the only star in this field of view in the *STEREO* data base. The variability of Y Sco was detected and its period determined by virtue of the blending effect with this star, about 2.4 pixel away. The overlaid dark circles illustrate the photometric aperture of the HIs, which is slightly different for each imager, at 3.2 pixel for *STEREO*/HI-1A and 3.1 pixel for *STEREO*/HI-1B (Bewsher et al. 2010). The galaxy with a bright core just below Y Sco has not been recorded.

Figure 5. Histogram showing the distribution of the proportional errors in the periods observed by *STEREO*/HI-1 using PDM (Stellingwerf 1978).

what is expected, as shown by the distribution of the known periods of Miras from Kharchenko & Kilpio (2000) displayed in the left-hand panel in Fig. 10. This is believed to be the result of the way the sample was selected, with a visual examination of large numbers of light curves: periods in this range would have a less distinctive pattern in the light curve and be almost impossible to distinguish from systematic effects.

The distribution of colours of known Miras from Kharchenko & Kilpio (2000) shows two main populations (Fig. 11, left) when comparing the $B1 - R1$ colours from Monet et al. (2003) against the $J - K$ colours from Skrutskie et al. (2006). The distribution of colours of stars in this sample observed by *STEREO*/HI-1 is very different, however (Fig. 11, right). This may in part reflect that it includes some semiregular variables but might also indicate that some of the stars in the sample have unusual features, such as circumstellar dust shells, or that they could have been misclassified. Checking the $B2 - I$ colours against $J - K$, from the same sources, shows a population of objects (Fig. 12, left) which is a better match for the

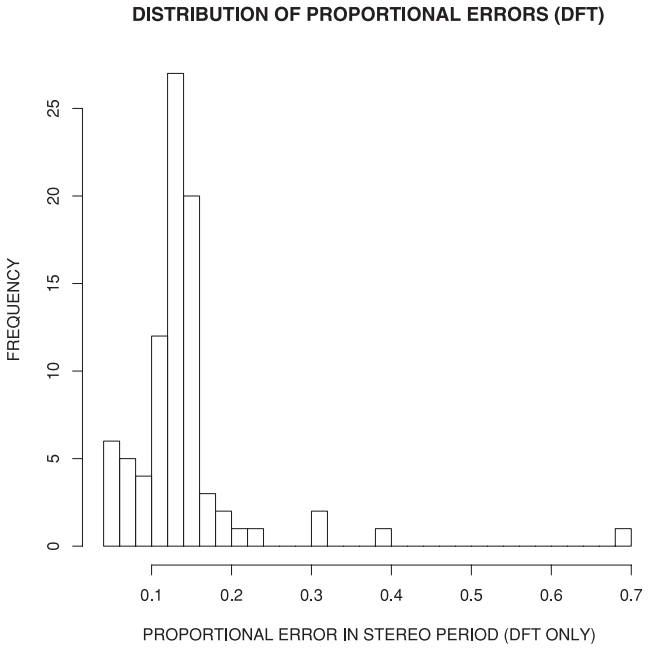

Figure 6. Histogram showing the distribution of the proportional errors in the periods observed by *STEREO*/HI-1 using a DFT (Deeming 1975).

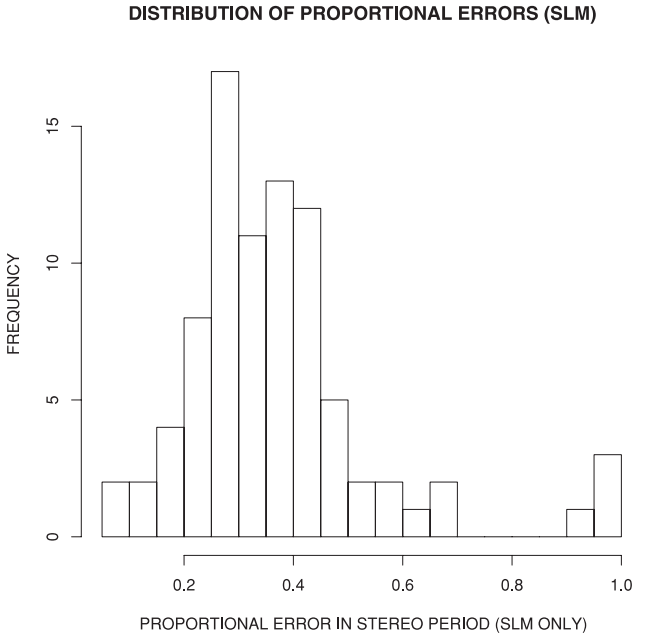

Figure 7. Histogram showing the distribution of the proportional errors in the periods observed by *STEREO*/HI-1 using SLM (Renson 1978).

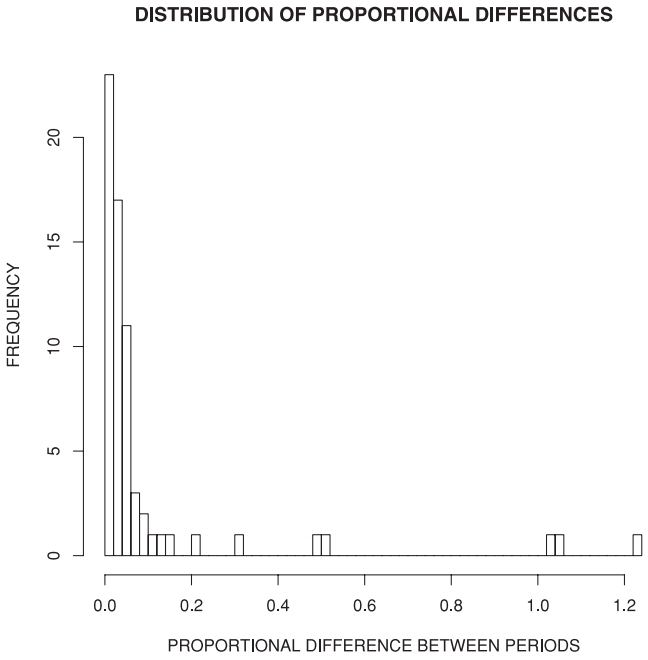

Figure 8. Histogram showing the distribution in the proportional differences $[(P_{\rm STEREO} - P_{\rm GCVS})/P_{\rm GCVS}]$ between the *STEREO*/HI-1 periods and those found in the literature (preferentially Samus et al. 2012).

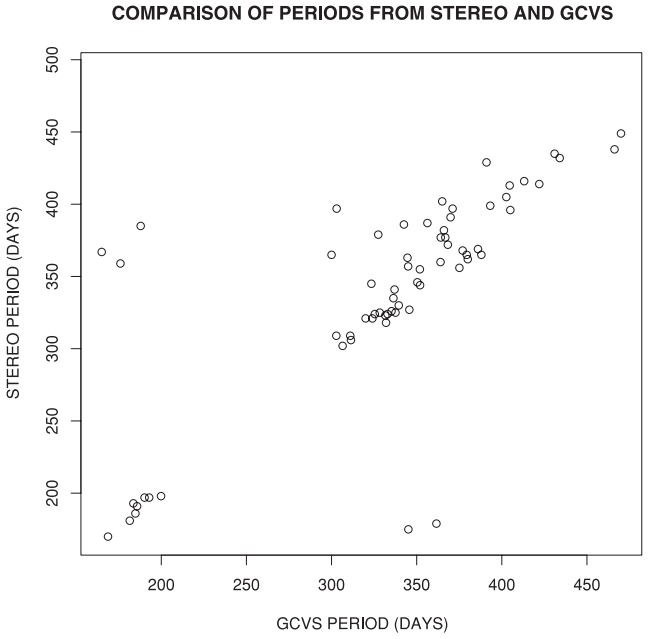

Figure 9. Plot comparing the periods observed by *STEREO*/HI-1 to those found in the literature (preferentially Samus et al. 2012).

sample observed by *STEREO*/HI-1 (Fig. 12, right). A slight bias for new and unclassified objects to have large $B2 - I$ is expected as a result of checking for Mira-like colours (i.e. very red objects) when attempting to ascertain the source of variability; however, it was not expected that the known Miras found would share this feature. The throughput of the *STEREO*/HI-1 imagers at about 950 nm is more likely to be responsible, as these objects are bright in the I band.

4 NOTES ON INDIVIDUAL STARS

This section details *STEREO*/HI-1 observations of particular stars of individual interest. To clarify the observations of those stars without a prior period determination, unfolded light curves are given for all the new candidates (Fig. 13), all the previously unclassified variables (Fig. 14) and the remaining stars for which a period has

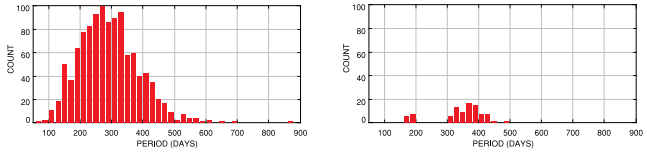

Figure 10. Histograms comparing the periods of known Mira variables from Kharchenko & Kilpio (2000), shown on the left, with the distribution of periods found for all variables in this work (right). The lack of periods between 200 and 300 d in this work is believed to be due to a selection effect, with periods in this range being more difficult to distinguish from systematic effects.

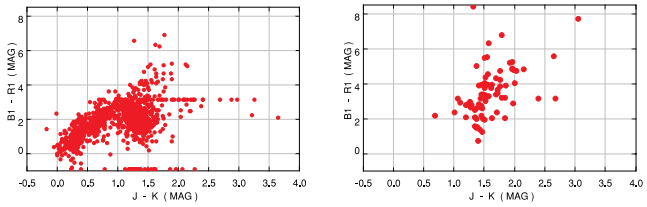

Figure 11. Plot of the $B1 - R1$ colours (Monet et al. 2003) against $J - K$ colours (Skrutskie et al. 2006) for all the Miras in Kharchenko & Kilpio (2000), left, and all the stars in this sample observed by *STEREO*/HI-1, right. V2055 Sgr, a known Mira, is the star with the largest value of $B1 - R1$ in our sample, whilst V718 Tau, also a known Mira, has the second-largest value of $B1 - R1$ and the largest value of $J - K$.

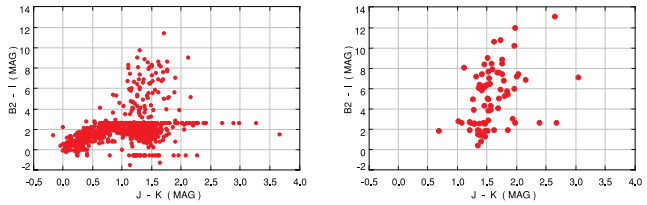

Figure 12. Plot of the $B2 - I$ colours (Monet et al. 2003) against $J - K$ colours (Skrutskie et al. 2006) for all the Miras in Kharchenko & Kilpio (2000), left, and all the stars in this sample observed by *STEREO*/HI-1, right. The stars with $(B2 - I) > 10$ from the *STEREO*/HI-1 sample are IK Tau, IRC −20507, 2MASS J19291709−2034504, OP Sgr and FQ Sgr, in decreasing order.

not previously been determined (Fig. 15). A few general comments about the observations are also worth noting.

(i) The times of maxima observed do not always correspond to the periods given in Table 1. This is because the times of maxima, the shape and amplitude of the light curve can all potentially change from cycle to cycle and the algorithms do not always give a good fit.

(ii) The shape of the light curve at maximum can sometimes be very flat, such that the star appears constant for many days, even longer than a single epoch of observations (about 20 d). In these cases, no maximum was recorded as it was not possible to determine a central time of maximum with an estimate of the error. Therefore, only those maxima sharply defined enough to produce an error of about 5 d or less were recorded.

(iii) In cases where the *STEREO*/HI-1 period found is a harmonic of the known period, it is difficult to know which is genuine, especially for those with periods near to a year or a fraction thereof. It would be necessary to combine all available observations to be sure for these stars but, although this is beyond the scope of the present paper, due to the relatively small number of data points herein we are not questioning the accuracy of periods given in the literature.

(iv) Classifications for the new LPV candidates, or previously unclassified variables, cannot be accurately determined as the magnitude of variability in the non-standard *STEREO*/HI-1 bandpass is not straightforward to convert to a more standard filter. In comparison to the brighter, better known Miras, however, it is likely that most are semiregular variables, if genuine. The reddening for many of the new candidates, some recorded as having circumstellar envelopes, is an additional complication.

(v) For 19 stars in the sample, the period presented here constitutes the first determination of a period. The irregular nature of these variables and the large errors in the periods require that these are taken with caution, individually, although for those stars with a known period there is general good agreement with the periods found here and thus there should also be similarly good agreement, overall, with those for which no period has previously been reported.

4.1 New candidate and unclassified variables

There are six candidate LPVs in the sample not listed as variables in the GCVS or its NSV supplement (Samus et al. 2012) and a further seven are listed as variables but not classified. Owing to the difficulties in determining the amplitude of variability, it is not possible to ascertain whether these are Miras or semiregular variables; however, given their apparent magnitudes and the lack of prior measurements or detection of their variability, it is perhaps more likely that most are semiregular variables. In particular, the sample was selected partly by the colours shown in Zacharias et al. (2004) and are very red objects, thus the likely classifications are limited to Miras and semiregular variables. As five of the new candidates were detected indirectly through blending with a nearby star, their light curves were also individually extracted using the coordinates provided by SIMBAD, in order to confirm the new sources are accurate. The light curves of all the new candidates are thus presented in Fig. 13, along with a constant star for comparison (HD 1651), demonstrating that large amplitude variability has genuinely been observed in these stars. Note that the constant star has a small difference in the observed magnitudes between *STEREO*/HI-1A and *STEREO*/HI-1B but that this is of the order of 50 mmag and that it remains constant for each satellite.

The new candidate LPVs are as follows.

(i) *IRAS 16482−2039*. There are probable systematic effects confusing the behaviour near minima. Nevertheless, the amplitude of variability clearly exceeds 1 mag. Only the region near minimum brightness and the decline from maximum are observed, as to be expected for a star with a period close to the orbital period of the *STEREO*-Behind satellite. This star is recorded as an IR source by *IRAS* (Neugebauer et al. 1984) and has no mention of variability. It also appears in the *Akari* FIS All-sky Survey Point Source Catalogue (Yamamura et al. 2010) and has fluxes at 65, 90 and 140 μm, the flux at 140 μm being equivalent to a magnitude of about 7.6, with the other two bands registering a magnitude of about 9.9. It was observed to show SiO masing in Deguchi et al. (2004), which implies that it is an evolved O-rich star undergoing mass loss.

(ii) *IRAS 17289−1917*. This star has either sharp maxima or maxima of varying brightness between epochs, although the minima appear smooth. The period is very close to one year and any variability could thus easily have been difficult or impossible to observe prior to the *STEREO*/HI-1 observations. It is recorded as an IR source by *IRAS* and features in Skrutskie et al. (2006) but it does

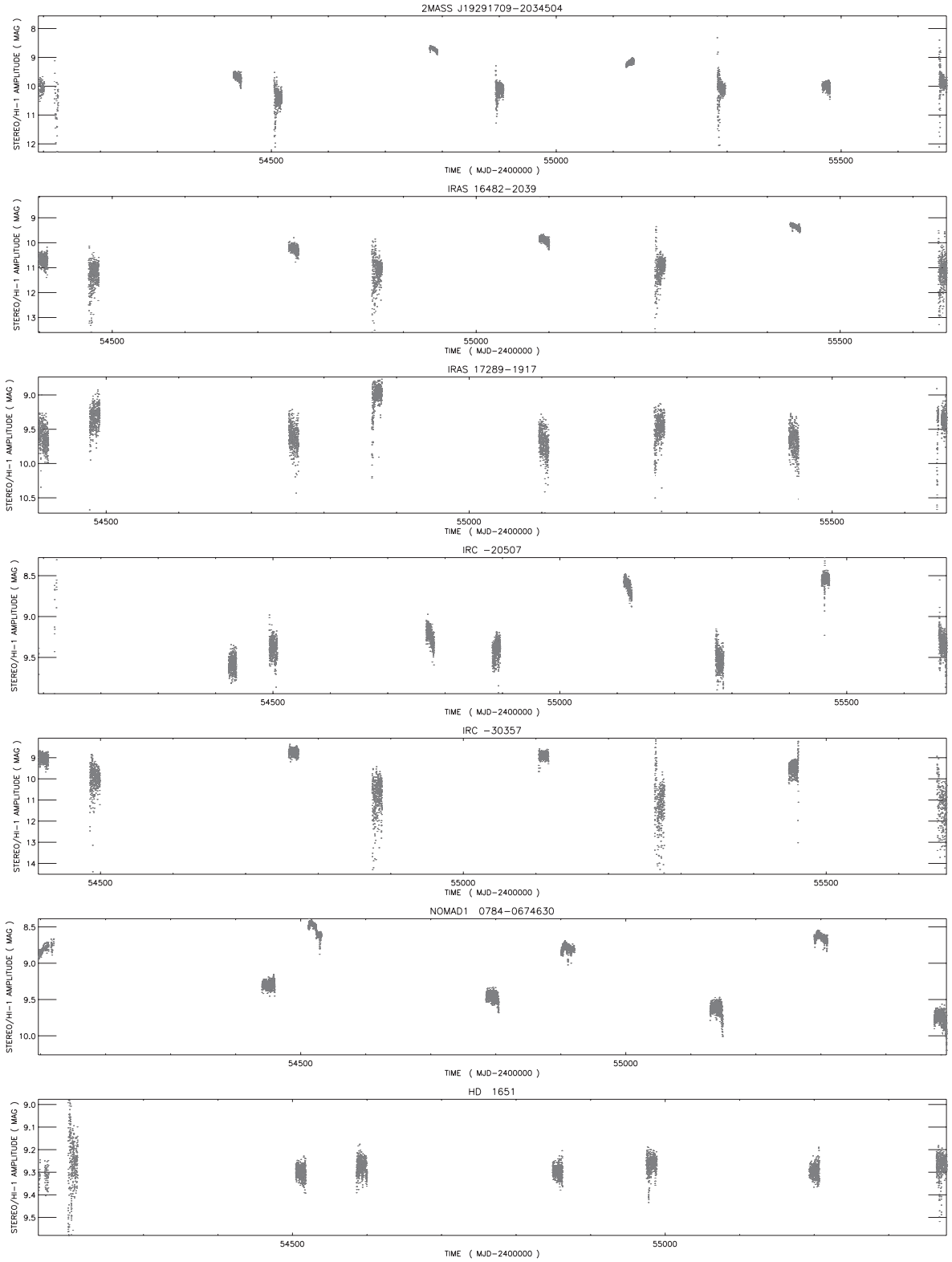

Figure 13. Unfolded light curves of the new candidate LPVs. The data shown here were extracted for their coordinates as given in SIMBAD for those detected indirectly through the pipeline described in Section 2.3 (all except NOMAD1 0784−0674630) and a constant star for comparison (HD 1651). The clear variability seen here further confirms that such indirect detections are able to recover the large amplitude signals of Miras and semiregular variables. Note that the constant star shows a small discrepancy between the *STEREO*/HI-1A and *STEREO*/HI-1B data but this is not on the scale of variability seen in the stars in our sample of LPVs and it also remains constant in each satellite's data, unlike the stars in our sample.

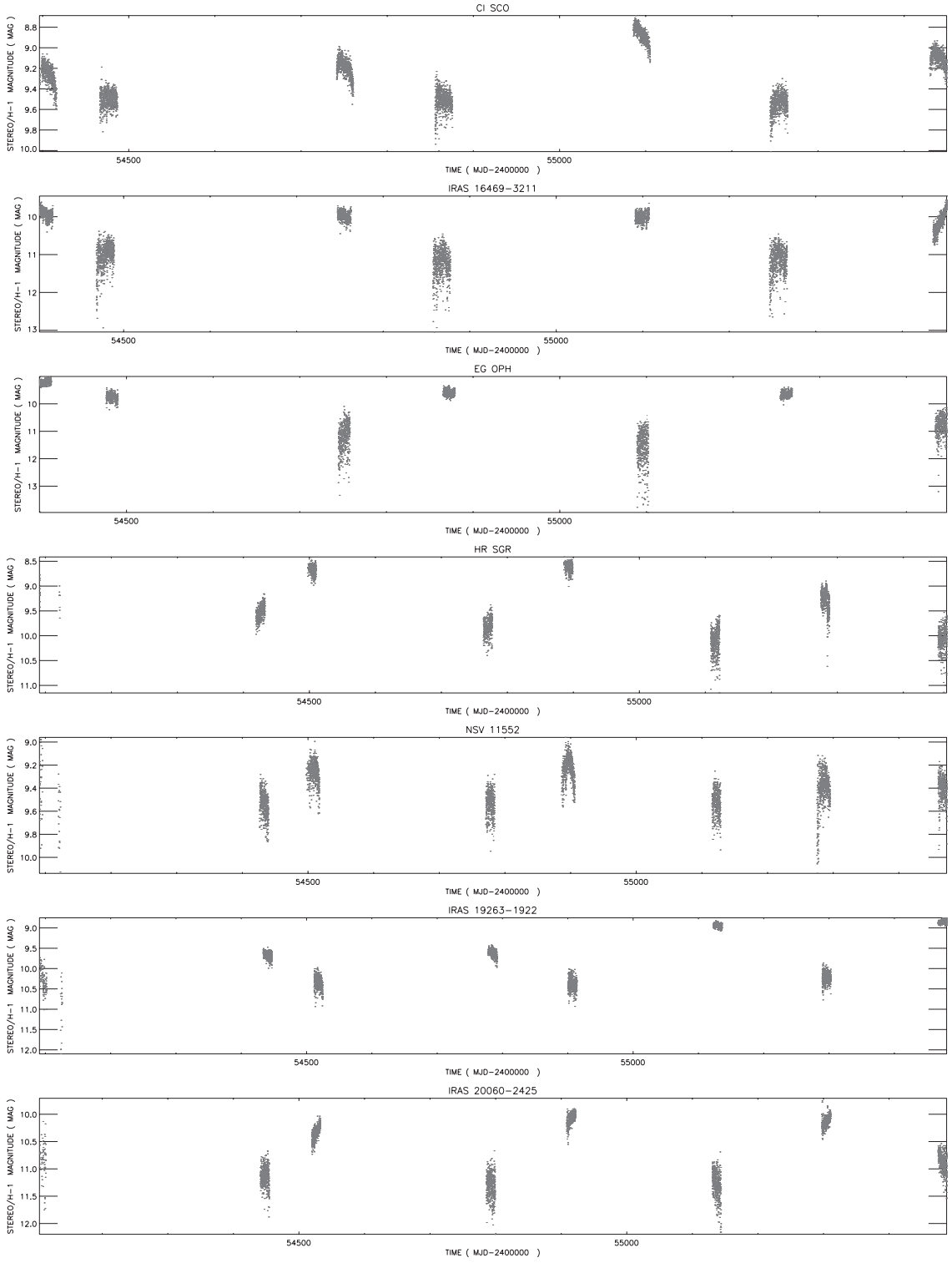

Figure 14. Unfolded light curves of the unclassified LPVs.

not appear in Yamamura et al. (2010) and has not been the subject of further investigation.

(iii) *IRC −30357*. This star shows extremely large amplitude variability but is hampered by the fact that it encroaches on the faint limit observable by *STEREO*/HI-1. It is possible that only the maxima are seen and that the star is too faint to observe at other times. The brightness of maximum may be variable between cycles. The star has been observed by *IRAS* and has been assigned a spectral type of M8, although there is no mention of variability and it does not appear in Yamamura et al. (2010). The *STEREO*/HI-1 data also show other variability with a period visually near 1 d, probably a result of blending with a nearby star possessing rotational variability, although none is recorded as such.

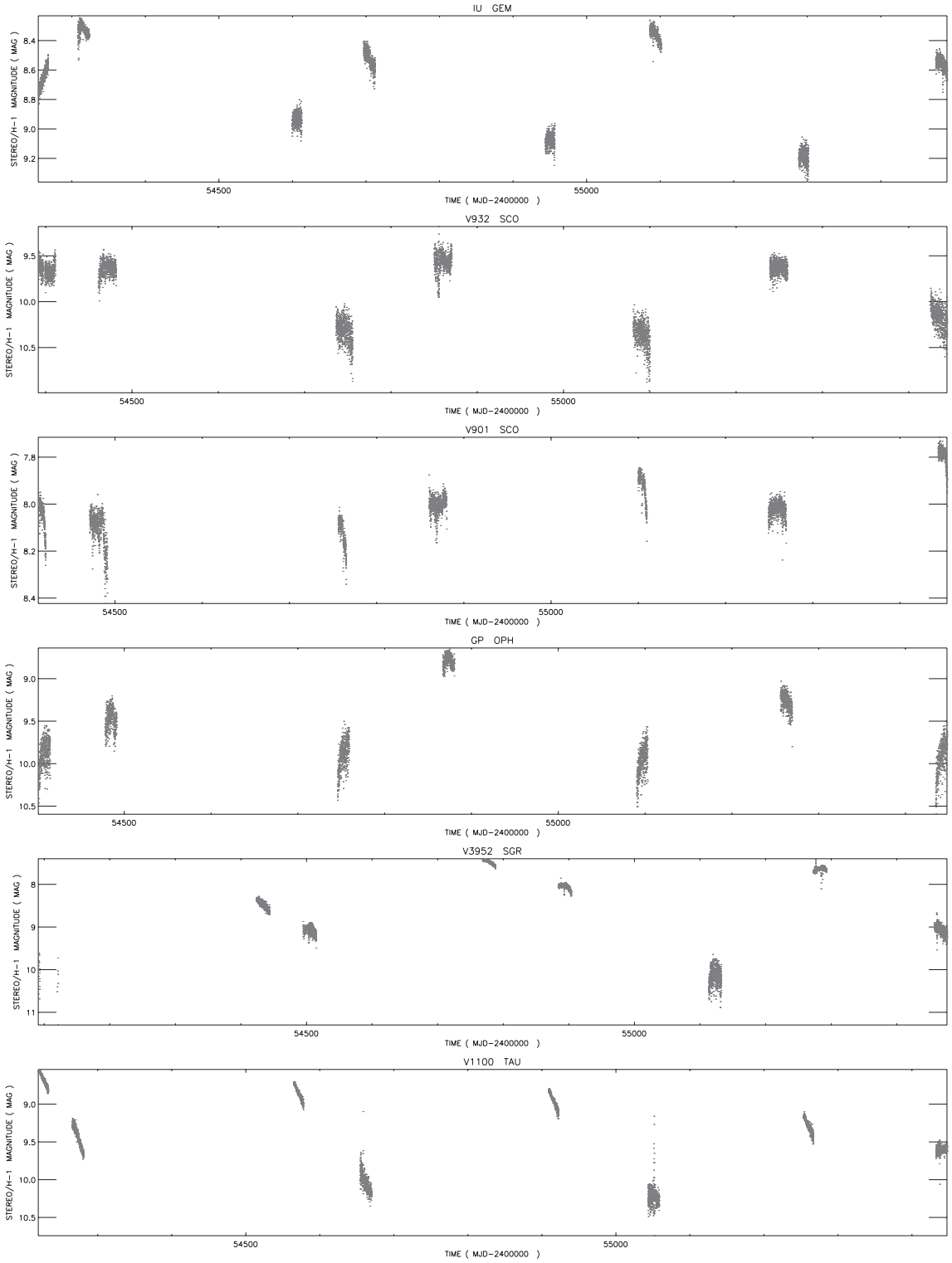

Figure 15. Unfolded light curves of the previously known variables for which the period found here is the first to be determined.

(iv) *IRC −20507*. The phase-folded light curve is relatively smooth for this star but it is unclear if there is a change in the brightness of maxima and minima between cycles. One maximum is observed but it is possible a second was just caught in the previous cycle, in which case the period given here of 431 d may be very wrong, with the most recent cycle having about 352 d between adjacent maxima. This would then be a sign of irregular variability or a significant period change. OH masing has been observed in this star (te Lintel Hekkert et al. 1991) and we therefore expect it to have a circumstellar envelope, making it a particularly interesting target for future study. The large value of $B2 - I$ (Monet et al. 2003), second only to IK Tau, is suggestive of the obscuring presence of a circumstellar envelope. The star is designated spectral type M7 in SIMBAD. In Yamamura et al. (2010), this star has fluxes at 65 and

90 μm, with equivalent magnitudes of 6.4 and 7.15, respectively. Variability with a periodicity visually near 1 d is also seen in the data, likely due to blending with a rotational variable, although none is recorded as such nearby.

(v) *2MASS J19291709−2034504*. No maxima are observed for this star but there are indications that the brightness of maximum could be variable. The star is listed in SIMBAD as spectral type M7 but very few observations have been made and no indication of variability is mentioned. The extremely large value of $B2 - I$ (Monet et al. 2003) is the third largest in the sample, after IK Tau and IRC −20507, which suggests that this star may host a circumstellar envelope. Follow-up observations to check for maser activity would be required to confirm this.

(vi) *NOMAD1 0784−0674630*. This star shows an erratic unfolded light curve and the median period of 381 d indicates that the shape and brightness of maxima and minima may be variable. There were no candidate sources near the observed coordinates other than this star that are likely to be Miras, with two other sources very nearby in Zacharias et al. (2004), of which one has colours resembling an A-type star and the other a large proper motion typical of a red dwarf. Another red star almost 3 arcmin away is less likely to be the source, TYC 5733-2876-1 (NOMAD1 0784−0674475), owing to its distance, magnitude and the magnitude of variability observed, although it should not be excluded from consideration.

The previously unclassified variables (their unfolded light curves are shown in Fig. 14) are as follows.

(i) *CI Sco*. The *STEREO*/HI-1A data appear to show a systematic trend that may be potentially confusing the period determination, although all the *STEREO*/HI-1B data appear to be at or very near minimum, consistent with the period being close to the orbital period of the *STEREO*-Behind satellite. There is some other variability observed in the light curve with a period visually near 5 d, although it is not clear in which star this originates. Although the variability is unclassified and no period is given, an amplitude of 1.5 mag has been recorded (Samus et al. 2012), which is about twice that observed by *STEREO*/HI-1.

(ii) *IRAS 16469−3211*. Poor phase coverage for this star contributes to an uncertainty in both the period and, given the uncertainties in the differences in the magnitudes seen by the two satellites, the overall amplitude. One epoch of data clearly shows a sharp increase in brightness and the phase-folded light curve places this close to the maximum in phase. This star is recorded as having an envelope of OH/IR type as a result of observations reported in te Lintel Hekkert et al. (1991) in which OH masing was detected. It was previously observed by *IRAS* but there is no mention of variability. The actual source observed by *STEREO*/HI-1 is nearby (NOMAD1 0577−0577145) and has very red colours also and there is a chance that this star may be the variable, if it is itself a Mira (however, it has no known variability of its own or observations other than photometry).

(iii) *EG Oph*. For this star the phase-folded light curve is smooth except for the first epoch of *STEREO*/HI-1A data, which might indicate a brighter maximum for that cycle. No period or classification has been determined for this star but the amplitude is reported as 1.4 mag (Samus et al. 2012). It has been observed to be an SiO maser source (Deguchi et al. 2004). There is a risk of contamination from EI Oph, approximately 3 pixel away in *STEREO*/HI-1, which has the same amplitude but is fainter and even more poorly observed.

(iv) *HR Sgr*. No period or classification is given in the GCVS or NSV (Samus et al. 2012); however, the given amplitude of 4.2 mag is suggestive of a Mira. The amplitude observed by *STEREO*/HI-1 of about 1.5 mag is not unusual in the context of the known Miras in this sample. There are indications that the signal seen is blended with a variable resembling a WUMa-type eclipsing binary, although this would not be expected to produce variability on the scale of a Mira. The median period found here is close to the orbital period of the *STEREO*-Behind satellite but the smoother parts of the phase-folded light curve are from the *STEREO*-Ahead satellite, so a systematic is less likely than changing brightness of the maxima between cycles.

(v) *NSV 11552*. This star has the lowest amplitude of variability in the sample and also one of the shortest periods. The amplitude, however, is given in SIMBAD as 1.7 mag, so this is unlikely to be rotational variability. It is unclear from the *STEREO*/HI-1 data whether the period might instead be twice that given here. Some other variability due to blending is evident in the light curve, although the source is uncertain. The two brightest stars in R nearby have significant proper motions indicative of red dwarf stars rather than Miras.

(vi) *IRAS 19263−1922*. The *STEREO*/HI-1 data are ambiguous regarding the maximum brightness, which might also be influencing the period determination. This star was observed to be an SiO maser source in Deguchi et al. (2007) and was noted for having a highly unusual radial velocity relative to the local standard of rest, possibly a dynamical effect due to the influence of the Galactic bulge bar (Deguchi, Shimoikura & Koike 2010). This star was observed in all four wavelengths by *Akari*/FIS, with equivalent magnitudes in 65, 90, 140 and 160 μm of about 8.2, 9.7, 8.2 and 7.7, respectively. Some other variability is evident in the light curve, possibly due to the nearby variable NSV 12065, this having a period visually between 1 and 2 d.

(vii) *IRAS 20060−2425*. There are indications of changing brightness of maxima between cycles for this star. The star has been observed by *IRAS* but is otherwise very poorly observed, although there is a possibility that the nearby AN 958.1936, recorded as variable in Luyten (1937), could have been an observation of it, or that the *STEREO*/HI-1 observations have detected the variability of this star.

4.2 Y Sco: flare-like event or starspot?

A recent search of data from the *CoRoT* mission found at best a tentative sign of a single flare-like event (Lebzelter 2011) in only one star. The larger sample we present here has the difficulty that many potential flares could easily be mistaken for a de-pointing event caused by a micrometeorite impact. Y Sco, however, displays an event that does not look like any of the known systematics and therefore might be a flare, although the time-scale of this feature, being of about 1 d duration, is longer than might be expected (Fig. 16). The feature begins in the first epoch of *STEREO*/HI-1B data, at MJD 245 4480 and lasts for 1 d , during which the brightness increases in a linear fashion by 0.1 mag. There is no change in the scatter of the light curve during this time, thus it is not due to a

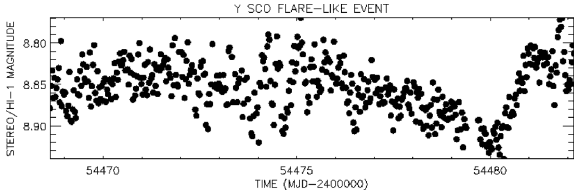

Figure 16. A candidate flare-like event (begins at MJD 245 4480) seen in Y Sco by *STEREO*/HI-1B.

micrometeorite hit. An alternative explanation for this feature might be that it is due to a dark spot on the surface rotating out of view, or perhaps a bright spot rotating into view. The star is only a few days away from maximum brightness at the time this event occurs. There is a remark in the GCVS (Samus et al. 2012) that this star has been irregular since 1972 and although the period observed by *STEREO*/HI-1 of 355 d is very similar to the pre-1972 period of 351.88 d, the interval between the two observed maxima is about 782 d. If the flare-like event is really due to a starspot, it might also mean that the maximum observed a few days before this was not a full maximum, and the star was still approaching maximum brightness.

Some caution needs to be taken with the variability, as the star actually observed by *STEREO*/HI-1 is NOMAD1 0706−0340442, 2.4 pixel away. There is very vague short period variability with a period visually close to a day in the light curve, with an amplitude of <50 mmag that may be from this star and its colours in Zacharias et al. (2004) are suggestive of a star of spectral type G or K. It thus has some potential for rotational variability and flares and spots of its own, although no other indication of such an event is seen in the light curve. If it has a rotational period near 1 d, this would likely exclude it as the source of the flare-like event, since this lasts about as long as one such rotation and could not be due to an event on a part of the surface of this star rotating into or out of view. There is an unrecorded galaxy with a bright core very close to Y Sco (RA: 247.°356; Dec. −19.°3638) but this is probably too faint for any active galactic nucleus type effects to be observed by *STEREO*/HI-1.

4.3 Period changing variables

15 of the stars in the sample are recorded in Samus et al. (2012) as showing variable periods. Column 9 of Table 1 labels these with a 1. These stars are briefly discussed here for indications of further period changes or other unusual features. Below this list, two other stars showing evidence of period changes are detailed.

(i) *V Tau*. This star has the shortest period among those found in the sample, at 170 d. This is a very good match to the known period of 168.7 d, thus no sign of period changing is observed.

(ii) *Z Tau*. This star has the second longest previously known period of any in the sample, at 466.2 d, whilst the period found here is just outside the typical 4 per cent difference, at 438 d. The accuracy of the period determination is unable to exclude a small period change but a significant change is unlikely.

(iii) *U Ori*. The period found here of 372 d is a good match to the known period of 368.3 d. The period is probably constant for the duration of the *STEREO*/HI-1 observations.

(iv) *T CMi*. The period found here of 325 d is a very good match to the known period of 328.3 d. A change in the shape between cycles is suggested by the phase-folded light curve, although a period change might also manifest in this way and not be picked up; thus, it is inconclusive for this star whether or not any change has occurred.

(v) *S Leo*. The period found here of 197 d is in fair agreement with the known period of 190.16 d. There is evidence of a small change in the brightness of maxima between cycles. Two successive maxima are observed with an interval of 186.3 d between them; within the errors of the times of maxima no period change is, therefore, found.

(vi) *SS Vir*. The period found here of 377 d is within the typical 4 per cent away from the known period of 364.14 d. Two successive maxima are observed with 342.14 d between them, suggesting a period decrease, however. The phase-folded light curve is not smooth and a period change or irregularity could have resulted in a poor period determination.

(vii) *S Vir*. The *STEREO*/HI-1 period of 356 d is slightly different from the 375.1 d from Samus et al. (2012) and the poor phase coverage may be hampering the period determination. It is therefore uncertain if the period is changing; however, the brightness of both maxima and minima might also be changing, which would further complicate the analysis.

(viii) *S Lib*. The period from *STEREO*/HI-1 of 197 d is in good agreement with the known period of 192.9 d and it seems unlikely that significant period changes have occurred. The phase-folded light curve nevertheless clearly shows that the brightness of maxima and possibly the shape of the light curve may differ from cycle to cycle.

(ix) *Y Sco*. See discussion in Section 4.2.

(x) *R Oph*. In spite of the large uncertainty in the period, the *STEREO*/HI-1 period of 302 d is in good agreement with the known period of 306.5 d. There is an indication of the brightness of minima varying between cycles but no indication of a significant period change.

(xi) *V1869 Sgr*. The *STEREO*/HI-1 period of 318 d only moderately agrees with the known period of 332 d and the phase coverage is poor as there is less data than normal for this star, likely due to it being so near to the edge of the field of view it may have been missed completely on some orbits. The analysis is therefore unable to determine if there have been any period changes.

(xii) *V3876 Sgr*. The period found here of 344 d is in good agreement with the known period of 352 d. A period change therefore seems unlikely. There is some indication of a change in maximum brightness between cycles.

(xiii) *RX Sgr*. The period found here of 326 d is in reasonable agreement with the known period of 335.23 d. An additional complication here is the presence of the known semiregular variable BH Sgr about 95 arcsec away. Changes in maximum brightness between cycles indicated by the light curve are therefore unreliable and it is uncertain what effect this other variable would have on the observations of the period, although with a period from Samus et al. (2012) of 100 d and being a much fainter object, the effects of RX Sgr should dominate.

(xiv) *AN Sgr*. The period found here of 325 d agrees moderately well with the known period of 337.56 d. The phase coverage is mostly concentrated around minimum and there is therefore no evidence of period changing or other significant differences between cycles.

(xv) *RR Sgr*. The period found here of 335 d is in excellent agreement with the known period of 336.33 d. The period is therefore unlikely to be significantly changing; however, the unfolded light curve indicates differences in maximum brightness and possibly shape between cycles.

Two other stars show evidence of a different period from that given in Samus et al. (2012). Both are classified as semiregular variables rather than Miras. Their unfolded light curves are shown in Fig. 17. Unfortunately, both are too poorly observed from the ground for the observations to be confirmed – no data for them exist in the online archives of the American Association of Variable Star Observers (AAVSO), the British Astronomical Association: Variable Star Section (BAAVSS) or the Association Française des Observateurs d'Étoiles Variables (AFOEV). Their position on the ecliptic plane makes long-term monitoring difficult, and without long-term monitoring it is impossible to ascertain whether the

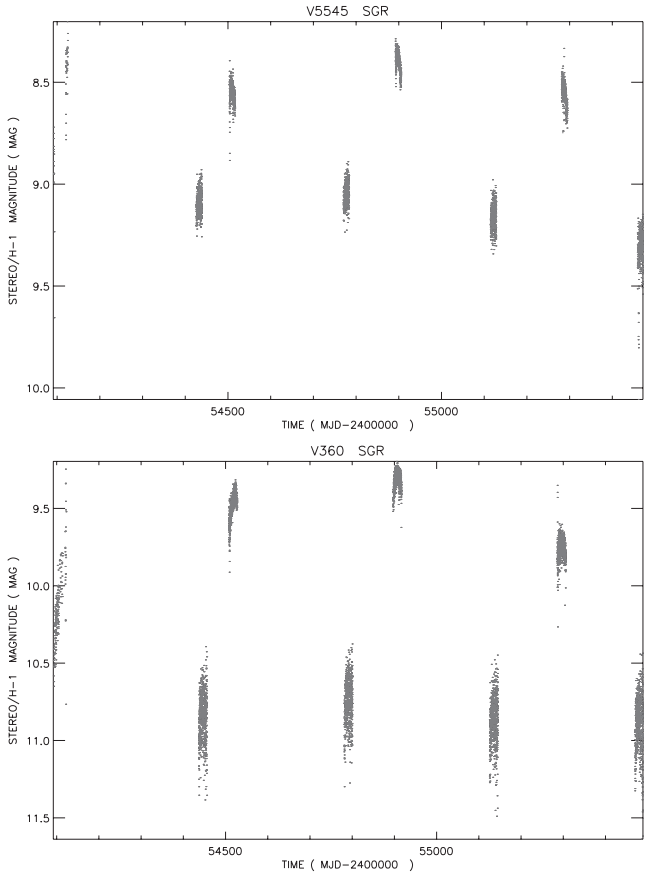

Figure 17. The unfolded *STEREO*/HI-1 light curves of V5545 Sgr (upper) and V360 Sgr (lower). Maxima for V5545 Sgr are observed at (times are MJD − 240 0000) 54506.99 ±2.5, 54895.71 ±3.0 and 55283.38 ±3.0. Maxima for V360 Sgr are observed at (times are MJD − 240 0000) 54506.99 ±2.5, 54895.71 ±3.0 and 55283.38 ±3.0.

periods are actively changing or meandering about a more regular value (Zijlstra & Bedding 2002). The two stars are as follows.

(i) *V5545 Sgr*. Although the period found here of 368 d is in reasonable agreement with the known period of 377 d, the three consecutive times of maximum brightness observed indicate a period of about 388 d (Fig. 17, upper plot). A small period change may therefore have occurred.

(ii) *V360 Sgr*. The period found here of 367 d is, at best, a very rough approximation of a harmonic of the known period of 165 d. The three maxima observed are not consistent with either period, being separated by 383.47 and 389.39 d (Fig. 17, lower plot). A significant period change may therefore have occurred, or the period may be irregular.

5 DISCUSSION

The arrangement of two almost identical cameras on almost identical satellites in different heliocentric orbits permits the observation of periodicity on time-scales not observable from the Earth or from a single satellite alone. The unusual bandpass of the *STEREO*/HI-1 instruments, in particular the throughput in the IR at about 950 nm (Fig. 1), allows for the observation of stars of very late spectral type and also for stars that are obscured by circumstellar dust shells. Together, this provides homogenous observations of Mira variables with improved phase coverage and has potentially detected some new objects of this type or the related semiregular class.

Even though some objects have either no *R* magnitude listed in Zacharias et al. (2004) or are fainter than the cut-off of 12th magnitude used to select objects to be observed by *STEREO*/HI-1, the large pixel scale of 70 arcsec nevertheless allows them to have an indirect influence on the light curves of very nearby stars that are in the *STEREO*/HI-1 data base (Fig. 4). Although in some regions, the Galactic Centre especially, it is difficult or impossible to ascertain the likely source of variability, the very large amplitudes and very long periods of Miras and semiregular variables are sufficiently distinctive that in some cases the variability is reliably observed even in a densely populated field of view. In the case of new candidate variables, it further complicates the matter of classification, which is essentially impossible from *STEREO*/HI-1 data alone, although it is likely most are of the semiregular class.

The majority of the sample of 85 stars are known Mira variables, with a small minority classified as semiregular variables and a single variable of the Orion type. Seven are listed as variable in either the GCVS or NSV (Samus et al. 2012) but without a classification, and six have not been previously observed to be variable. For 19 stars, the period we present here is the first determination of a period. There is a reasonable agreement between the periods previously known and those found by an analysis of the *STEREO*/HI-1 photometry (Fig. 9), although a harmonic is occasionally found and also some of the stars are known to change their periods. The accuracy of the period determination is insufficient to detect small changes in period of a few days but larger changes of a couple of weeks are potentially observable (Fig. 8). The new candidate and unclassified variables are individually discussed, as are those known or suspected of period changing. One star showing a particularly unusual feature is discussed: Y Sco, which shows a candidate flare-like event, although a starspot might also be an alternative explanation (Fig. 16).

Of the newly discovered variables, two (IRC −20507 and 2MASS J19291709−2034504) have exceptionally large values of $B2 - I$ (Fig. 12). This may be suggestive of the presence of a circumstellar envelope and these stars might be therefore potential maser sources; indeed IRC −20507 has already been recorded as such (te Lintel Hekkert et al. 1991). Follow-up observations of these stars would contribute to the understanding of the evolution of stars during the AGB stage. There are features of some stars of this type that cannot be explained by current models, such as an excess of ammonia (Menten et al. 2010) and subsolar values of $^{16}O/^{17}O$ and $^{16}O/^{18}O$ (Decin et al. 2010), and having more examples to study would be very useful. We encourage interested readers to make follow-up observations of the new candidate variables, in order to confirm their nature and periodicity. To assist in this, we provide dates when the new candidate variables will be observed by *STEREO*/HI-1 so that observations may be conducted simultaneously (Table 2). It is hoped that five years' worth of *STEREO*/HI-1 data will soon be made available for all stars in the field of view with listed *R* magnitudes of 12 or greater in the NOMAD1 catalogue (Zacharias et al. 2004), although a date has not yet been fixed. In due course, more data will be gathered by *STEREO*/HI but it is not known when, or even if, this will be made available on a large scale.

A complete lack of objects with periods between 200 and 300 d is observed in the sample (Fig. 10, right). There are a small number found with periods that are over 400 d; thus, it cannot be completely excluded that one or more of those may in fact be harmonics with a genuine period in this range. Nevertheless, for a sample of this size, this is a significant feature and the only likely explanation is that it is the result of a selection effect. In the earliest stage

of the analysis, many thousands of light curves were visually examined in a search for long period variability; however, it is not easy to distinguish artificial effects from genuine variability, especially for stars with potentially very erratic variability in terms of the magnitude of maxima, minima, shape and even period. This may have caused genuine variables with periodicity in this range to be too unconvincing to have been recorded as a likely variable. A similar selection effect might also have led to a preference for finding variables with periods near 1 yr or close to the orbital periods of the two *STEREO* satellites as these produce a more recognizable pattern in the unfolded light curves. It is therefore likely that more Miras and semiregular variables remain undiscovered in the data.

A selection effect may also be responsible for the prevalence of stars in our sample with large $B2 - I$ values from Monet et al. (2003), shown in the right-hand panel in Fig. 12. The search for the sources of variability was focused on very red objects, although other colours are also given in Zacharias et al. (2004), in particular the *J*, *H* and *K* colours from Skrutskie et al. (2006). This prevalence could also be partly due to the sensitivity of the *STEREO*/HI-1 imagers at about 950 nm (Fig. 1), making it easier to recover variability from stars bright at this wavelength.

The photometry gathered by *STEREO*/HI-1 on both long and short time-scales of bright stars on the ecliptic plane is a valuable resource for the observation and monitoring of Miras and semiregular variables. Some variables of this type have periods close to a year, or a fraction thereof, and the full range of their behaviour cannot be monitored from Earth or Earth orbit and thus the homogenous observations of *STEREO*/HI-1 provide a unique window to advance the study of these poorly understood objects.

ACKNOWLEDGMENTS

The HI instrument was developed by a collaboration that included the Rutherford Appleton Laboratory and the University of Birmingham, both in the UK, and the Centre Spatial de Liége (CSL), Belgium, and the US Naval Research Laboratory (NRL), Washington DC, USA. The *STEREO*/SECCHI project is an international consortium of the Naval Research Laboratory (USA), Lockheed Martin Solar and Astrophysics Lab (USA), NASA Goddard Space Flight Center (USA), Rutherford Appleton Laboratory (UK), University of Birmingham (UK), Max-Planck-Institut für Sonnensystemforschung (Germany), Centre Spatial de Liége (Belgium), Institut d'Optique Théorique et Appliquée (France) and Institut d'Astrophysique Spatiale (France). This research has made use of the SIMBAD data base, operated at CDS, Strasbourg, France. This research has made use of NASA's Astrophysics Data System. This research has made use of the statistical analysis package R (R Development Core Team 2008). This publication makes use of data products from the 2MASS, which is a joint project of the University of Massachusetts and the Infrared Processing and Analysis Center/California Institute of Technology, funded by the National Aeronautics and Space Administration and the National Science Foundation. This research has made use of version 2.31 Peranso light curve and period analysis software, maintained at CBA, Belgium Observatory (http://www.cbabelgium.com). This research is based on observations with *Akari*, a JAXA project with the participation of ESA. This research is funded by the Science and Technology Facilities Council (STFC). KTW acknowledges support from an STFC studentship. This research was funded by the Austrian Science Fund (FWF): P21988-N16 and AP2300621. The authors wish to thank Dr Luca Fossati of the Open University for useful conversations.

REFERENCES

Bewsher D., Brown D. S., Eyles C. J., Kellett B. J., White Glenn J., Swinyard B., 2010, Sol. Phys., 264, 433
Bewsher D., Brown D. S., Eyles C. J., 2012, Sol. Phys., 276, 491
Brown D. S., Bewsher D., Eyles C. J., 2009, Sol. Phys., 254, 185
Davis C. J. et al., 2012, MNRAS, 420, 1355
Decin L. et al., 2010, A&A, 521, L4
Deeming T. J., 1975, Ap&SS, 36, 137
Deguchi S. et al., 2004, PASJ, 56, 765
Deguchi S. et al., 2007, PASJ, 59, 559
Deguchi S., Shimoikura T., Koike K., 2010, PASJ, 62, 525
Eyles C. J. et al., 2009, Sol. Phys., 254, 387
Fluks M. A., Plez B., The P. S., de Winter D., Westerlund B. E., Steenman H. C., 1994, A&AS, 105, 311
Groenewegen M. A. T., Blommaert J., 2005, A&A, 443, 143
Hoffleit D., 1997, J. Am. Assoc. Var. Star Obser., 25, 115
Ita Y. et al., 2004, MNRAS, 347, 720
Kaiser M. L., Kucera T. A., Davila J. M., St. Cyr O. C., Guhathakurta M., Christian E., 2008, Space Sci. Rev., 136, 5
Kharchenko N. V., Kilpio E., 2000, Balt. Astron., 9, 646
Lattanzio J. C., Wood P., 2004, in Habing H. J., Olofsson H., eds, Asymptotic Giant Branch Stars. Springer-Verlag, Berlin, p. 23
Lebzelter T., 2011, A&A, 530, 35
Lebzelter T., Andronche S., 2011, Inf. Bull. Var. Stars, 5981, 1
Lorenz D., Lebzelter T., Nowotny W., Telting J., Kerschbaum F., Olofsson H., Schwarz H. E., 2011, A&A, 532, A78
Luyten W. J., 1937, Astron. Nachr., 261, 451
Matsunaga N., Fukushi H., Nakada Y., 2005, MNRAS, 364, 117
Menten K. et al., 2010, A&A, 521, L7
Monet D. G. et al., 2003, AJ, 125, 984
Murakami H., Meixner M., Fraser O., Srinivasan F., Cook K., Vijh U., 2007, PASJ, 59, 369
Neugebauer G. et al., 1984, ApJ, 278, L1
Nowotny W., Aringer B., Höfner S., Lederer M. T., 2011, A&A, 529, A129
Olivier E. A., Wood P. R., 2005, MNRAS, 362, 1396
R Development Core Team, 2008, R: A Language and Encironment for Statistical Computing. R Foundation for Statistical Computing, Vienna, Austria
Rejkuba M., 2004, A&A, 413, 903
Renson P., 1978, A&A, 63, 125
Riebel D., Meixner M., Fraser O., Srinivasan F., Cook K., Vijh U., 2010, ApJ, 723, 1195
Samus N. N. et al., 2012, General Catalogue of Variable Stars (GCVS data base, Version 2012Jan) CDS B/gcvs
Skrutskie M. F. et al., 2006, AJ, 131, 1163
Stellingwerf R., 1978, ApJ, 224, 953
te Lintel Hekkert P., Caswell J. L., Habing H. J., Haynes R. F., Haynes R. F., Norris R. P., 1991, A&AS, 90, 327
Templeton M. R., Mattei J. A., Willson L. A., 2005, AJ, 130, 776
Uttenthaler S. et al., 2011, A&A, 531, A88
Whitelock P., Marang F., Feast M., 2000, MNRAS, 319, 728
Whitelock P., Feast M., van Leeuwen F., 2008, MNRAS, 386, 313
Wood P. R., 2000, Publ. Astron. Soc. Aust., 17, 18
Wraight K. T., White Glenn J., Norton A. J., Bewsher D., 2011, MNRAS, 416, 2477
Wraight K. T., Fossati L., Netopil M., Paunzen E., Rode Paunzen M., Bewsher D., Norton A. J., White Glenn J., 2012, MNRAS, 420, 757
Yamamura I., Makiuti S., Ikeda N., Fukuda Y., Oyabu S., Koga T., White Glenn J., 2010, VizieR On-line Data Catalog, II/298
Zacharias N., Monet D., Levine S., Urban S., Gaume R., Wycoff G., 2004, BAAS, 36, 1418
Zijlstra A. A., Bedding T. R., 2002, J. Am. Assoc. Var. Star Obser., 31, 2

SUPPORTING INFORMATION

Additional Supporting Information may be found in the online version of this article:

Appendix A. The phase-folded light curves for all 85 stars in the sample are shown in Figs A1–A5. In each case, the period folded on is shown in the title, along with some other information on the star for ease of reference.

Please note: Wiley-Blackwell are not responsible for the content or functionality of any supporting materials supplied by the authors. Any queries (other than missing material) should be directed to the corresponding author for the article.

This paper has been typeset from a TEX/LATEX file prepared by the author.